Trapping analysis of a magnetized electron by a circularly polarized electromagnetic wave in static electric field

Abstract

A pseudo-potential model is developed to investigate a previously unexplored velocity trapping mechanism arising from anomalous Doppler resonance when a magnetized electron interacts simultaneously with a circularly polarized electromagnetic wave and a static electric field. When the wave amplitude exceeds a critical threshold, the electron's parallel velocity becomes trapped and oscillates within a pseudo-potential well, while energy supplied by the static electric field is continuously converted into gyrokinetic energy. Numerical simulations demonstrate the formation of a stable trapping region and identify the threshold conditions required for trapping. The resulting energy transfer ratio from the static electric field to the gyrokinetic energy is quantified and shown to be in good agreement with predictions from quantum theory.

I. Introduction

Wave–particle interactions play a central role in plasma physics and are widely exploited for both particle acceleration and confinement. Through appropriate resonance conditions, electromagnetic waves can exchange energy and momentum efficiently with charged particles, leading to a broad range of phenomena in laboratory plasmas, fusion devices, and space environments.

In the context of particle acceleration, one of the most well-known mechanisms is autoresonance, in which a charged particle maintains phase synchronism with an electromagnetic wave through nonlinear effects. A representative example is the gyro-resonant accelerator[1-3], where electrons interact resonantly with a fixed-frequency electromagnetic wave in a slowly varying magnetic field, allowing the relativistic mass increase to compensate for changes in the cyclotron frequency. Other acceleration mechanisms include betatron resonance[4-6] and ponderomotive-force-driven acceleration[7, 8]. Velocity-space acceleration may also occur through Landau resonance, in which particles become trapped in the potential well of a longitudinal wave, subsequent variation of the wave phase velocity can then lead to sustained particle acceleration[9].

Particle trapping, on the other hand, is commonly associated with spatial confinement mechanisms, such as optical tweezers or ponderomotive potential wells formed by the interference of electromagnetic waves[10]. In plasma environments, trapping in velocity space has been observed in a variety of wave–particle interactions, including nonlinear interactions between electrons and chorus waves[11], electromagnetic ion cyclotron (EMIC) waves[12], and whistler-mode waves[13]. These processes are of particular importance in both space plasmas and magnetic confinement devices, where they influence particle transport, energy redistribution, and radiation emission.

Despite extensive studies of charged particle interactions with electromagnetic and electrostatic waves in magnetized plasmas[14-22], most theoretical treatments consider electromagnetic waves while ignoring the effects of static electric fields. [23, 24]. The combined effect of a static electric field and an electromagnetic wave under a background magnetic field has received comparatively little attention, even though such configurations naturally arise in systems such as tokamak plasmas, where strong toroidal electric fields coexist with wave activity, and in space plasmas, where large-scale electric fields accompany wave–particle interactions. In these environments, static electric fields are known to play a critical role in runaway electron generation[25] and pitch-angle scattering[11] [26], suggesting that their interaction with resonant wave dynamics warrants further investigation.

In this work, we extend the relativistic pseudo-potential framework originally developed by Bellan [14] to study pitch-angle scattering by circularly polarized electromagnetic waves, explicitly incorporating a static electric field parallel to the background magnetic field. We demonstrate that, under anomalous Doppler resonance, the presence of a static electric field gives rise to a previously unexplored velocity trapping mechanism. When the wave amplitude exceeds a critical threshold, the electron's parallel velocity becomes trapped and oscillates within a pseudo-potential well, while energy continuously supplied by the static electric field is converted into gyrokinetic energy. This energy conversion sustains the resonance condition and leads to stable trapping in velocity space.

The trapping dynamics and threshold conditions are investigated numerically, and the resulting energy transfer from the static electric field to the gyrokinetic energy is quantified. The numerical results are further benchmarked against predictions from quantum theory, showing good agreement and confirming the consistency between classical dynamics and quantum descriptions of anomalous Doppler resonance. These findings suggest potential implications for runaway electron control and wave-based plasma heating mechanisms.

The remainder of this paper is organized as follows. In Section II, we develop the theoretical framework describing the interaction between a magnetized electron, a circularly polarized electromagnetic wave, and a static electric field. Section III presents numerical simulations of the trapping dynamics and analyzes the conditions required for trapping. In Section IV, the classical results are compared with quantum theoretical predictions. Section V discusses the physical interpretation and potential applications of the trapping mechanism, and Section VI summarizes the main conclusions.

II. electron-electromagnetic wave interaction analysis

2.1 Field equations

To analyze interaction between electron and E.M wave, we consider an E.M wave propagating along uniform magnetic field whose phase velocity $\mathrm{v_T} = \omega/\mathrm{k}$, where ω is the angular frequency and k is the wavenumber. The uniform background magnetic field is $B_o = B_o\hat{z}$. The wave's magnetic field perturbation $\tilde{B}$ is characterized by the dimensionless parameter $\kappa \equiv |\tilde{B}|/B_o$, such that the total magnetic field becomes $\mathbf{B} = B_0\hat{z} + \tilde{B}$. The system includes a static electric field $E_o = E_o\hat{z}$, with the total electric field given by $\mathbf{E} = E_0\hat{z} + \tilde{E}$, where $\tilde{E}$ represents the electric field components of E.M wave:

$$\tilde{\mathbf{E}} = \mathrm{E_w}\left[\hat{x}\cos(\mathrm{kz} - \omega \mathrm{t}) + g\,\hat{y}\sin(\mathrm{kz} - \omega \mathrm{t})\right] \tag{1}$$

Here, $\mathrm{E_w}$ is the electric field amplitude of E.M wave, and the polarization satisfies the left-hand circular polarization (LCP) condition when g = 1, and right-hand circular polarization (RCP) condition when g = -1.

Faraday's law requires the associated magnetic field to be

$$\widetilde{\boldsymbol{B}} = \frac{k}{\omega}\hat{z} \times \widetilde{\boldsymbol{E}} = \kappa B_0[-g\,\hat{x}\sin(kz-\omega t) + \hat{y}\cos(kz-\omega t)] \tag{2}$$

Here $\kappa B_0 = \mathrm{B_w} = \frac{\mathrm{k}}{\omega} E_w$.

2.2 Transformation to the wave frame

In wave frame, which denotes as prime and moves at constant velocity $\mathrm{v_T} = \omega/\mathrm{k}$ with respect to the lab frame, the fields are

$$E'_{\parallel} = E_{\parallel} \tag{3}$$

$$B'_{\parallel} = B_{\parallel} \tag{4}$$

$$E'_{\perp} = \gamma_T(\boldsymbol{E} + v_T \times \boldsymbol{B})_{\perp} \tag{5}$$

$$B'_{\perp} = \gamma_T\left(\boldsymbol{B} - \frac{1}{c^2} v_T \times \boldsymbol{E}\right)_{\perp} \tag{6}$$

Where $\gamma_T = 1/\sqrt{1-\left(\frac{v_T}{c}\right)^2}$. Substituting the wave fields Eq. (1), Eq. (2) into Eq.(5), Eq. (6) gives $E'_{\perp} = 0$ and $B'_{\perp} = \frac{B_{\perp}}{\gamma_T}$.

Since $\{\boldsymbol{k}, \frac{i\omega}{c}\}$ and $\{\mathbf{x}$, ict$\}$ are relativistic four-vectors, we have

$$kz - \omega t = k\gamma_T(z' + v_T t') - \omega\gamma_T\left(t' + \frac{v_T z'}{c^2}\right) = k'z' \tag{7}$$

Here $k' = k/\gamma_T$ and z' are the wavenumber and position in the wave frame. The magnetic field of E.M wave is

$$\boldsymbol{B}'_{\perp} = B'_{\perp}(-g\,\hat{x}\sin(k'z') + \hat{y}\cos(k'z')) \tag{8}$$

The motion equation of the charge particle in the prime frame is

$$\frac{d}{dt'}(\gamma'\beta') = \frac{q}{m}\left(\frac{E_0}{c}\hat{z} + \beta' \times B'\right) \tag{9}$$

Where $\gamma' = 1/\sqrt{1-\beta'^{\,2}}$, m is the rest mass of electron and q is the electron charge with q = -e. Note that γ,γ_T, and γ' differ and should not be confused with each other. The derivation of energy γ' to t' and the motion equation in each direction should be

$$\frac{d\gamma'}{dt'} = \frac{qE_0\hat{z}\cdot\beta'_z}{mc} \tag{10}$$

$$\frac{d}{dt'}(\gamma'\beta'_z) = \Omega\left(\frac{E_0}{cB_0}\hat{z} + \beta'_{\perp} \times \frac{B'_{\perp}}{B_0}\right) \tag{11}$$

$$\frac{d}{dt'}(\gamma'\beta'_{\perp}) = \Omega\left(\beta'_{\perp} \times \hat{z} + \beta'_z\hat{z} \times \frac{B'_{\perp}}{B_0}\right) \tag{12}$$

Here Ω is the nonrelativistic electron cyclotron frequency in the lab frame with $\Omega < 0$. Introduce

$$\xi_z = 1 + \alpha\gamma'\beta'_z \tag{13}$$

Here $\alpha = \frac{g\omega}{\Omega\gamma_T} n$. And

$$\xi_\perp = 1 + \alpha\gamma'\beta'_\perp \tag{14}$$

where $n = ck/\omega$, according to Eq. (11) , Eq. (12), we have

$$\frac{d\xi_z}{dt'} = \alpha\Omega\left(\frac{E_0}{cB_0}\hat{z} + \frac{\xi_\perp - 1}{\alpha\gamma'} \times \frac{B'_\perp}{B_0}\right)\cdot\hat{z} \tag{15}$$

$$\frac{d\xi_\perp}{dt'} = \alpha\Omega\left(\frac{\xi_\perp - 1}{\alpha\gamma'} \times \hat{z} + \frac{\xi_z - 1}{\alpha\gamma'}\hat{z} \times \frac{B'_\perp}{B_0}\right) \tag{16}$$

2.3 Construction of pseudo-potential equation

Taking the derivative of Eq. (15) with respect to t' gives

$$\frac{d^2\xi_z}{dt'^2} = \alpha\Omega\left(\frac{d}{dt'}\left(\frac{\xi_\perp - 1}{\alpha\gamma'}\right) \times \frac{B'_\perp}{B_0}\right)\cdot\hat{z} + \alpha\Omega\left(\frac{\xi_\perp - 1}{\alpha\gamma'} \times \frac{d}{dt'}\left(\frac{\boldsymbol{B}'_\perp}{B_0}\right)\right)\cdot\hat{z} \tag{17}$$

And

$$\frac{d}{dt'}\left(\frac{\xi_\perp - 1}{\alpha\gamma'}\right) = \frac{1}{\alpha\gamma'}\cdot\frac{d\xi_\perp}{dt'} - \frac{\xi_\perp - 1}{\alpha\gamma'^2}\frac{d\gamma'}{dt} \tag{18}$$

According to Eq. (10) and ξ_z, we have

$$\frac{d\gamma'}{dt'} = \Omega\frac{E_0}{B_0 c}\frac{\xi_z - 1}{\alpha\gamma'} \tag{19}$$

While in Eq. (29), assuming $\beta'_\perp \ll \beta'_z$ and $B'_\perp < B_0$,we obtain

$$\left|\frac{d\xi_\perp}{dt'}\right| < \left|\Omega\frac{\xi_z - 1}{\gamma'}\right| \tag{20}$$

Finally, in the right side of Eq. (18)

$$\frac{\left|\frac{\xi_\perp - 1}{\alpha\gamma'^2}\cdot\frac{d\gamma'}{dt'}\right|}{\left|\frac{1}{\alpha\gamma'}\cdot\frac{d\xi_\perp}{dt'}\right|} < \frac{E_0\beta'_\perp}{B_0 c} \tag{21}$$

While for $\beta'_\perp \ll 1$ and $|\frac{E_0}{B_0 c}| \ll 1$, we can confidently ignore the second term in the right side of Eq. (18), then

$$\frac{d}{dt'}\left(\frac{\xi_\perp - 1}{\alpha\gamma'}\right) = \frac{1}{\alpha\gamma'}\cdot\frac{d\xi_\perp}{dt'} \tag{22}$$

Combing Eq. (17) with Eq. (22) , we have

$$\frac{d^2\xi_z}{dt'^2} = \alpha\Omega\left(\frac{1}{\alpha\gamma'}\cdot\frac{d\xi_\perp}{dt'}\times\frac{B'_\perp}{B_0}\right)\cdot\hat{z} + \alpha\Omega\left(\frac{\xi_\perp - 1}{\alpha\gamma'}\times\frac{d}{dt'}\left(\frac{\boldsymbol{B}'_\perp}{B_0}\right)\right)\cdot\hat{z} \tag{23}$$

Substituting Eq. (29) into Eq. (23) gives

$$\frac{d^2\xi_z}{dt'^2} = \alpha\Omega\left[\frac{\Omega}{\gamma'}\left(\beta'_\perp\times\hat{z} + \beta'_z\hat{z}\times\frac{B'_\perp}{B_0}\right)\times\frac{B'_\perp}{B_0} + \beta'_\perp\times\frac{d}{dt'}\left(\frac{\boldsymbol{B}'_\perp}{B_0}\right)\right]\cdot\hat{z} \tag{24}$$

The time derivation of wave magnetic field in wave frame is

$$\frac{d\boldsymbol{B}'_\perp}{dt'} = -k'\frac{dz'}{dt'}B'_\perp(g\,\hat{x}\cos(k'z') + \hat{y}\sin(k'z') = g\omega n'\beta'_z\hat{z}\times\boldsymbol{B}'_\perp \tag{25}$$

where $n' = \frac{ck'}{\omega} = n/\gamma_T$. By substituting Eq. (25) into Eq. (24)(23) and simplify Eq. (24) gives

$$\frac{d^2\xi_z}{dt'^2} = \frac{\alpha\Omega^2}{\gamma'}\left(\frac{\beta'_\perp\cdot\boldsymbol{B}'_\perp}{B_0}(1 + \frac{g\omega n}{\Omega\gamma_T}\gamma'\beta'_z) - \beta'_z\frac{\boldsymbol{B}'_\perp}{B_0}\cdot\frac{\boldsymbol{B}'_\perp}{B_0}\right) \tag{26}$$

Since $\xi_z = 1 + \frac{g\omega n}{\Omega\gamma_T}\gamma'\beta'_z$, finally

$$\frac{d^2\xi_z}{dt'^2} = \frac{\alpha\Omega^2}{\gamma'}\left(\frac{\beta'_\perp\cdot\boldsymbol{B}'_\perp}{B_0}\xi_z - \beta'_z\frac{\boldsymbol{B}'_\perp}{B_0}\cdot\frac{\boldsymbol{B}'_\perp}{B_0}\right) \tag{27}$$

2.3.1 connect $\frac{\beta'_\perp\cdot\boldsymbol{B}'_\perp}{B_0}$ with ξ_z

To obtain the relationship between $\frac{\boldsymbol{\beta}'_\perp\cdot\boldsymbol{B}'_\perp}{\boldsymbol{B_0}}$ and ξ_z, taking the time derivation of $\frac{\beta'_\perp\cdot\boldsymbol{B}'_\perp}{B_0}$ gives

$$\frac{\mathrm{d}}{\mathrm{dt}'}\left(\frac{\beta'_\perp\cdot\boldsymbol{B}'_\perp}{B_0}\right) = \frac{d\beta'_\perp}{dt'}\cdot\frac{\mathrm{B}'_\perp}{B_0} + \beta'_\perp\cdot\frac{d}{dt'}\left(\frac{\mathrm{B}'_\perp}{B_0}\right) \tag{28}$$

According to Eq. (10) and Eq. (12), we have

$$\frac{d\beta'_\perp}{dt'} = \Omega'\left(\beta'_\perp\times\hat{z} + \beta'_z\left(\hat{z}\times\frac{B'_\perp}{B_0}\right)\right) - \frac{\Omega' E_0\hat{z}\cdot\beta'_z}{cB_0}\beta'_\perp \tag{29}$$

Here $\Omega' = \Omega/\lambda'$. Substituting Eq. (29) into Eq. (28) gives

$$\frac{d\beta'_\perp}{dt'}\cdot\frac{\mathrm{B}'_\perp}{B_0} = -\hat{z}\cdot\left(\beta'_\perp\times\frac{B'_\perp}{B_0}\right)\Omega' - \Omega'\frac{E_0\beta'_z}{cB_0}\left(\beta'_\perp\cdot\frac{B'_\perp}{B_0}\right) \tag{30}$$

and

$$\beta'_\perp\cdot\frac{d}{dt'}\left(\frac{\mathrm{B}'_\perp}{B_0}\right) = \beta'_\perp\cdot g\omega n'\beta'_z\left(\hat{z}\times\frac{\boldsymbol{B}'_\perp}{B_0}\right) = -g\omega n'\beta'_z\left(\beta'_\perp\times\frac{\boldsymbol{B}'_\perp}{B_0}\right)\cdot\hat{z} \tag{31}$$

Finally, we have

$$\frac{\mathrm{d}}{\mathrm{d}t'}\left(\frac{\beta'_\perp\cdot\boldsymbol{B}'_\perp}{B_0}\right)=-\xi_z\Omega'\hat{z}\cdot\left(\beta'_\perp\times\frac{B'_\perp}{B_0}\right)-\Omega'\frac{E_0\beta'_z}{cB_0}\left(\frac{\beta'_\perp\cdot\boldsymbol{B}'_\perp}{B_0}\right) \tag{32}$$

The equation is first-order linear differential equation with the form:

$$\mathrm{T}'(\tau)+\mathrm{PT}(\tau)=\mathrm{Q}(\tau) \tag{33}$$

Where $\mathrm{P}=\frac{E_0\beta'_z}{cB_0}$, $\mathrm{Q}=-\xi\hat{z}\cdot\left(\beta'_\perp\times\frac{B'_\perp}{B_0}\right)$ and $\tau=\mathrm{t}'\Omega'$. The exact solution of z is

$$\mathrm{T}=\mathrm{e}^{-\int\mathrm{Pd\tau}}*\left[\iint e^{\int Pd\tau'}Qd\tau+C_0\right] \tag{34}$$

Since |P|<< 1 in most case of Tokamak environment, we have

$$\mathrm{T}=\int Qd\tau \tag{35}$$

Here we choose the initial condition $|\beta'_{\perp 0}|\ll 1$, which implies C_0 = 0. As a result, the expression Eq. (32) can simplify to:

$$\frac{\mathrm{d}}{\mathrm{d}t'}\left(\frac{\beta'_\perp\cdot\boldsymbol{B}'_\perp}{B_0}\right)=-\xi_z\Omega'\hat{z}\cdot\left(\beta'_\perp\times\frac{B'_\perp}{B_0}\right) \tag{36}$$

The substitution of Eq. (15) into Eq. (36) gives

$$\frac{\mathrm{d}}{\mathrm{d}t'}\left(\frac{\beta'_\perp\cdot\boldsymbol{B}'_\perp}{B_0}\right)=-\xi_z\Omega'\left(\frac{1}{\alpha\Omega}\frac{d\xi_z}{dt'}-\frac{E_0}{cB_0}\right) \tag{37}$$

Integrating Eq. (37) with t′ gives:

$$\frac{\beta'_\perp\cdot\boldsymbol{B}'_\perp}{B_0}=-\frac{\xi_z^2-{\xi_z}_0^2}{2\alpha\gamma'}+\frac{E_0}{cB_0}\int\xi_z\Omega'dt'+\frac{\beta'_{\perp 0}\cdot\boldsymbol{B}'_{\perp\mathbf{0}}}{B_0} \tag{38}$$

Here ξ_{z0}, $\beta'_{\perp 0}$ and $\boldsymbol{B}'_{\perp\mathbf{0}}$ represent the initial condition of ξ_z, $\beta'_\perp$ and $\boldsymbol{B}'_\perp$.

Noting that t = 0 corresponds to z'=0, since z = 0 at t= 0, and recalling the four vectors {γβ, γ}, we have the relation:

$$\gamma'_0\beta'_{\perp 0}=\gamma_0\beta_{\perp 0} \tag{39}$$

Since $\mathrm{B}'_{\perp 0}$ is in the y direction when z′ = 0 as shown in Eq. (8), it follows that

$$\frac{\beta'_{\perp 0}\cdot\boldsymbol{B}'_{\perp\mathbf{0}}}{B_0}=\frac{\beta'_{y0}B'_\perp}{B_0}=\frac{\gamma_0}{\gamma'_0}\kappa'\beta_{\perp 0}\sin\phi_0 \tag{40}$$

Where ϕ_0 is defined by $\beta_{x0}=\beta_{\perp 0}cos\phi_0$ and $\beta_{y0}=\beta_{\perp 0}\sin\phi_0$, $\kappa'=\frac{\kappa}{\gamma_T}=\frac{B'_\perp}{B_0}$. With these definitions, Eq. (38) becomes

$$\frac{\beta'_\perp\cdot\boldsymbol{B}'_\perp}{B_0}=-\frac{\xi_z^2-{\xi_z}_0^2}{2\alpha\gamma'}+\frac{E_0}{cB_0}\int\xi_z\Omega'dt'+\frac{\gamma_0}{\gamma'_0}\kappa'\beta_{\perp 0}\sin\phi_0 \tag{41}$$

The substitution of Eq. (41) into Eq. (27) gives:

$$\frac{d^2\xi_z}{dt'^2}=\frac{\alpha\Omega^2}{\gamma'}\left(\left(-\frac{\xi_z^2-\xi_{z0}^2}{2\alpha\gamma'}+\frac{E_0}{cB_0}\int\xi_z\Omega' dt'+\frac{\gamma_0}{\gamma_0'}\kappa'\beta_{\perp 0}\sin\phi_0\right)\xi_z-\beta_z'\kappa'^2\right) \tag{42}$$

Simplifying Eq. (42) and substituting ξ_z for β_z' gives:

$$\frac{d^2\xi_z}{dt'^2}=\Omega'^2\left(\xi_z\left(-\frac{\xi_z^2-\xi_{z0}^2}{2}+\frac{\varsigma E_0}{cB_0}\int\Omega'\xi_z dt'+\alpha\gamma_0\kappa'\beta_{\perp 0}\sin\phi_0\right)-(\xi_z-1)\kappa'^2\right) \tag{43}$$

Here

$$\varsigma = g\frac{\omega n}{\Omega\gamma_T}\gamma' \tag{44}$$

Normalization of time t' with $\tau = t'\Omega'$ we have

$$\frac{d^2\xi_z}{d\tau^2}=\left(\xi_z\left(-\frac{\xi_z^2-\xi_{z0}^2}{2}+\frac{\varsigma E_0}{cB_0}\int\xi_z d\tau+\alpha\gamma_0\kappa'\beta_{\perp 0}\sin\phi_0\right)-(\xi_z-1)\kappa'^2\right) \tag{45}$$

The Eq. (45)could also be written as

$$\frac{d^2\xi_z}{d\tau^2}=-\frac{\partial\psi}{\partial\xi_z} \tag{46}$$

Where

$$-\frac{\partial\psi}{\partial\xi_z}=\left(\xi_z\left(-\frac{\xi_z^2-\xi_{z0}^2}{2}+\frac{\varsigma E_0}{cB_0}\int\xi_z d\tau+\alpha\gamma_0\kappa'\beta_{\perp 0}\sin\phi_0\right)-(\xi_z-1)\kappa'^2\right) \tag{47}$$

Multiplying Eq. (46) by $d\xi_z/d\tau$ and integrating gives a pseudo-energy equation

$$\frac{1}{2}\left(\frac{d\xi_z}{d\tau}\right)^2+\psi(\xi_z)=W_0 \tag{48}$$

Where pseudo-potential equation is

$$\psi=\frac{1}{8}\xi_z^4+\left(\kappa'^2-\frac{\xi_{z0}^2}{2}-gs\kappa' sin\phi_0\right)\frac{\xi_z^2}{2}-\kappa'^2\xi_z-\int\xi_z\frac{\varsigma E_0}{cB_0}\int\xi_z d\tau d\xi \tag{49}$$

And

$$\mathrm{W}_0=\frac{1}{2}\left(\frac{d\xi_z}{d\tau}\right)^2|_{\tau=0}+\psi(\xi_{z0}) \tag{50}$$

Here $s=\frac{\omega n\beta_{\perp 0}\gamma_0}{\Omega\gamma_T}$.The pseudo potential ψ can only be solved numerically, as it does not have a regular form involving only the parameter ξ, here ψ also depends on t', which is related to β_z' and $\beta_\perp'$.

When $E_0=0$, the pseudo-potential equation reduces to

$$\psi=\frac{1}{8}\xi_z^4+\left(\kappa'^2-\frac{\xi_{z0}^2}{2}-gs\kappa' sin\phi_0\right)\frac{\xi_z^2}{2}-\kappa'^2\xi_z \tag{51}$$

which has the same expression as Eq. (41) in Ref. [14], as derived by P. M. Bellan.

2.4 Initial condition

From Eq. (15), we see that

$$\frac{d\xi_z}{d\tau} = g\left(\frac{\omega n}{\Omega\gamma_T}\kappa'\gamma\big(\beta_x\cos(kz-\omega t)+g\beta_y\sin(kz-\omega t\,)\big)\right)+\frac{\varsigma E_0}{cB_0} \tag{52}$$

Here, we use the relation $\gamma\beta_\perp = \gamma'\beta'_\perp$ and $\kappa' = B'_\perp/B_0$. At the initial time t = 0 and position z = 0, we have

$$\frac{d\xi_z}{d\tau}|_{\tau=0} = gs\kappa' cos\phi_0 + \frac{\varsigma E_0}{cB_0} \tag{53}$$

2.6 Solve $\boldsymbol{\beta}_\perp$

According to Eq.(12), multiplying $\gamma'\beta'_\perp$ on both sides gives

$$\frac{1}{2}\frac{d(\gamma'\beta'_\perp)^2}{dt'} = \Omega\gamma'\beta'_\perp\cdot\left(\beta'_z\times\frac{B'_\perp}{B_0}\right) \tag{54}$$

Reorganize the equation, we have

$$\frac{1}{2}\frac{d(\gamma'\beta'_\perp)^2}{dt'} = -\Omega\gamma'\beta'_z\cdot\left(\beta'_\perp\times\frac{B'_\perp}{B_0}\right) \tag{55}$$

According to Eq.(11), multiplying $\gamma'\beta'_z$ on both sides gives

$$\frac{1}{2}\frac{d(\gamma'\beta'_z)^2}{dt'} = \Omega\gamma'\beta'_z\cdot\left(\frac{E_0}{cB_0}\hat{z}+\beta'_\perp\times\frac{B'_\perp}{B_0}\right) \tag{56}$$

Add Eq. (55) and Eq. (56), we have

$$\frac{1}{2}\frac{d(\gamma'\beta'_\perp)^2}{dt'}+\frac{1}{2}\frac{d(\gamma'\beta'_z)^2}{dt'} = \frac{\Omega\gamma' E_0\beta'_z}{cB_0} \tag{57}$$

Which means energy change ratio equal to work done by static electric field in moving frame.

Using the normalized time $\tau = t'\Omega'$, we have

$$\frac{1}{2}\frac{d(\gamma'\beta'_\perp)^2}{d\tau}+\frac{1}{2}\frac{d(\gamma'\beta'_z)^2}{d\tau} = \frac{{\gamma'}^2 E_0\beta'_z}{cB_0} \tag{58}$$

Considering that γ' is mainly determined by β'_z, integrating both sides with t' gives

$$\beta'^2_\perp = \frac{2}{{\gamma'}^2|_t}\cdot\int_0^t \frac{{\gamma'}^2 E_0\beta'_z}{cB_0}d\tau + \left({\beta'_{z0}}^2+{\beta'_{\perp 0}}^2\right)-\beta'^2_z \tag{59}$$

III. Numerical study of the trapping effect

According to Eq. (46), Eq. (47) and Eq.(53), the velocity β'_z could be numerically solved by ode45, and $\beta'_\perp$ can be determined from Eq.(59). Then, using the four-vector $\{\gamma\beta,\gamma\}$, we have:

$$\gamma = \beta_T \gamma_T \gamma' \beta_z' + \gamma_T \gamma' \tag{60}$$

$$\beta_\perp = \frac{\gamma' \beta_\perp'}{\gamma} \tag{61}$$

$$\beta_z = \frac{\gamma_T \gamma'}{\gamma} (\beta_z' + \beta_T) \tag{62}$$

Finally, all the velocities in lab frame can be solved numerically

Quantum analysis indicates that, for anomalous Doppler resonance with electrons, the wave polarization is primarily dictated by the LCP component[27], whereas normal Doppler resonance corresponds to the RCP component. We begin by considering two cases in which a LCP electromagnetic wave interacts with electron in the presence of a uniform magnetic field and a static electric field.

In case I, considering a scenario where the uniform magnetic field B_0 = 2 T and the static electric field E_0 = −0.2 V/m, both along the z-axis, which are close to typical Tokamak plasma conditions. A plane LCP E.M wave is assumed to propagate along z direction with refractive index $n = 4$ where $\omega = 1.1\ \Omega$ and k = 1290 m^{-1}[28]. The electric field of E.M wave is set to $E_\omega = 20\ V/m$. The numerical results are shown in Figure 1, For the static electric field $E_0 < 0$, the direction of the electric field is opposite to that of the background magnetic field. As a result, the parallel velocity increases over time, as shown in Figure.1(a). Since here $\alpha < 0$, which is given in Eq. (13), the value of ξ_z decreases as β_z increase. When the parallel velocity satisfies the anomalous doppler resonance condition where $\xi_z = 0$, the perpendicular velocity $\beta_\perp$ increase abruptly, as shown in Figure.1 (b-d). After the parallel velocity exceeds the resonance condition, the $\beta_\perp$ will no longer increase. The phase evolution of ξ_z and $\frac{1}{\Omega'}\frac{d\xi_z}{dt'}$ is shown in fig.(e). It can be observed that the fluctuation of $\frac{1}{\Omega'}\frac{d\xi_z}{dt'}$ is stronger for $\xi_z < 0$ than for $\xi_z > 0$. This is because the change of $\frac{1}{\Omega'}\frac{d\xi_z}{dt'}$ is proportional to $\beta_\perp$ as shown in Eq. (52), An increase in $\beta_\perp$ therefore leads to stronger fluctuations in $\frac{1}{\Omega'}\frac{d\xi_z}{dt'}$. Fig 1.(f) illustrates the pseudo-potential $\Delta\psi(\xi)$, defined as $\Delta\psi(\xi) = \psi(\xi) - \psi(\xi_0)$ .The initial pseudo-kinetic energy $W_0 = \frac{1}{2}\left(\frac{d\xi_z}{dt'}\right)^2 |_{t'=0}$, which is indicated as red dash line in Fig.1 (f). The $\Delta\psi(\xi)$ cannot exceed W_0 due to the conservation of pseudo energy, as given in Eq. (48) , where the $\frac{1}{2}\left(\frac{d\xi_z}{d\tau}\right)^2 \geq 0$ must always be satisfied.

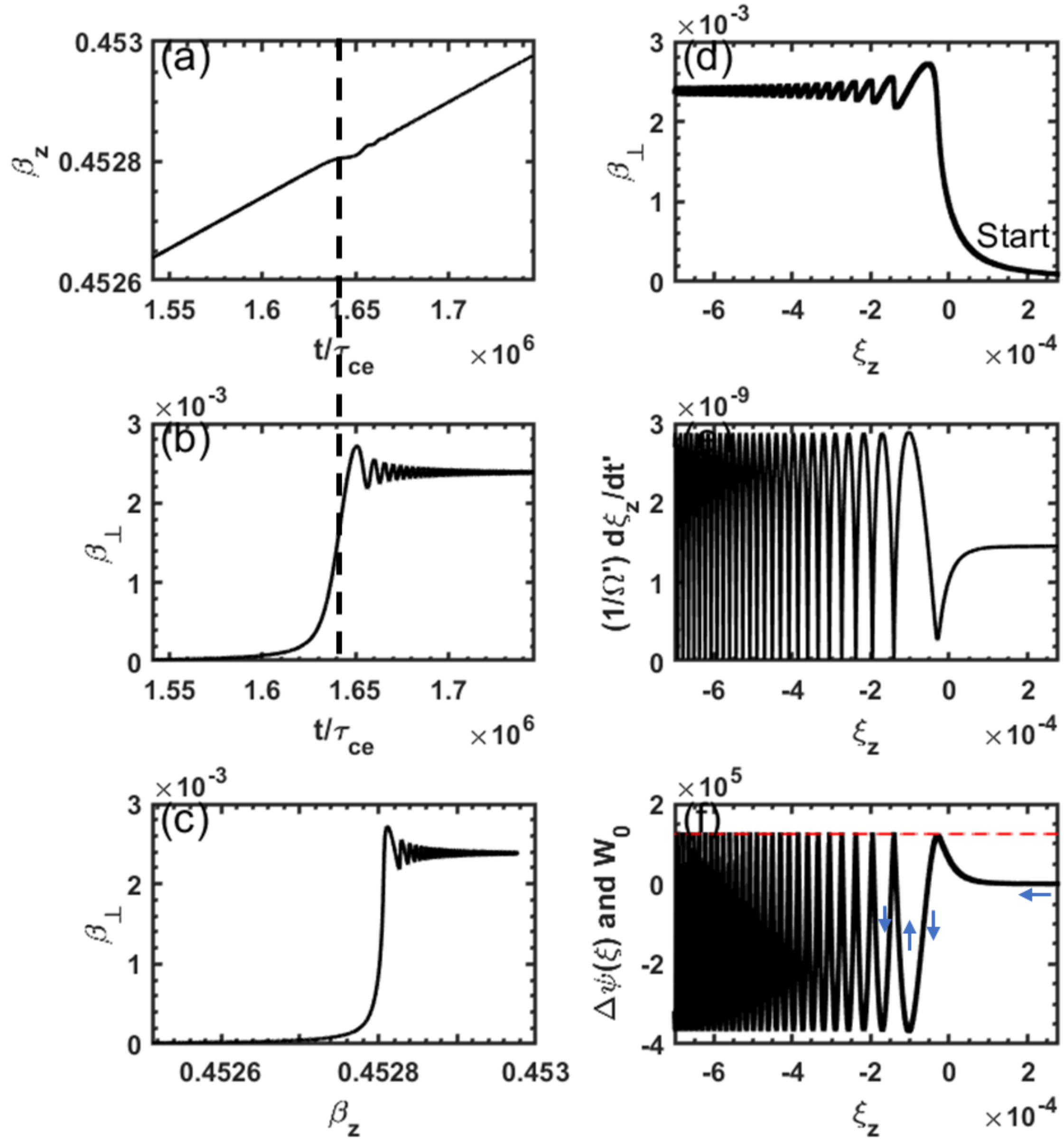

Figure 1. Numerical integration of Eq. (45) *with initial equation Eq.*(53)*. Input parameters are E_0=- 0.2 V/m, E_w = 20 V/m, B_0 = 2 T, $\omega/\Omega = -1.1$,g = 1, initial β_z= 0.45 and $\beta_\perp = 0$, $\phi_0 = 0$, n = 4. This give $\kappa' \approx 1.29 \times 10^{-7}, \gamma_T = 1.0308, \alpha = -4.373, \gamma_0 = 1.1198$ and $\gamma' = 1.0264, \frac{cE_0}{cB_0} = 1.458 \times 10^{-9}$. (a) The time evolution of β_z, here τ_{ce} refers to the cyclotron period of electron. (b) The time evolution of $\beta_\perp$.(c)The velocity phase in (β_z , $\beta_\perp$). (d)The evolution of $\beta_\perp$ with ξ_z. (e) The evolution of $d\xi_z/d\tau$ with ξ_z. (f)The pseudo-potential $\Delta\psi(\xi)$ (black line) and the initial pseudo-kinetic energy W_0 (red dash line)*

In case II, the electric field of the LCP E.M wave is increased to $E_\omega = 22\ V/m$. As the electron's parallel velocity approaches the resonant velocity, it no longer increases continuously but begins to oscillate around the resonant velocity, as shown in Fig. 2(a). While on the other hand, the perpendicular velocity increases continuously when β_z trapping in resonant region, as shown in Fig.2 (b-d). The phase trajectory of $(\xi_z, \frac{1}{\Omega'}\frac{d\xi_z}{dt'})$ is shown in Fig.2 (e). The closed-loop structure indicates periodic motion around the resonant point, and the direction of motion is labeled with arrow. The electron can only propagate within the region where the pseudo-potential $\Delta\psi(\xi)$ is lower than the initial pseudo-kinetic energy W_0. When the pseudo-potential tends to surpass the W_0, the electron velocity rebounds upon reaching the boundary of the pseudo-potential well. Consequently, the electron becomes confined within the well, the width of the pseudo-potential well also increases, since it is influenced by the parameter $\beta_\perp$. This bounce effect, shown in Fig.2 (f), illustrates the trapping phenomenon.

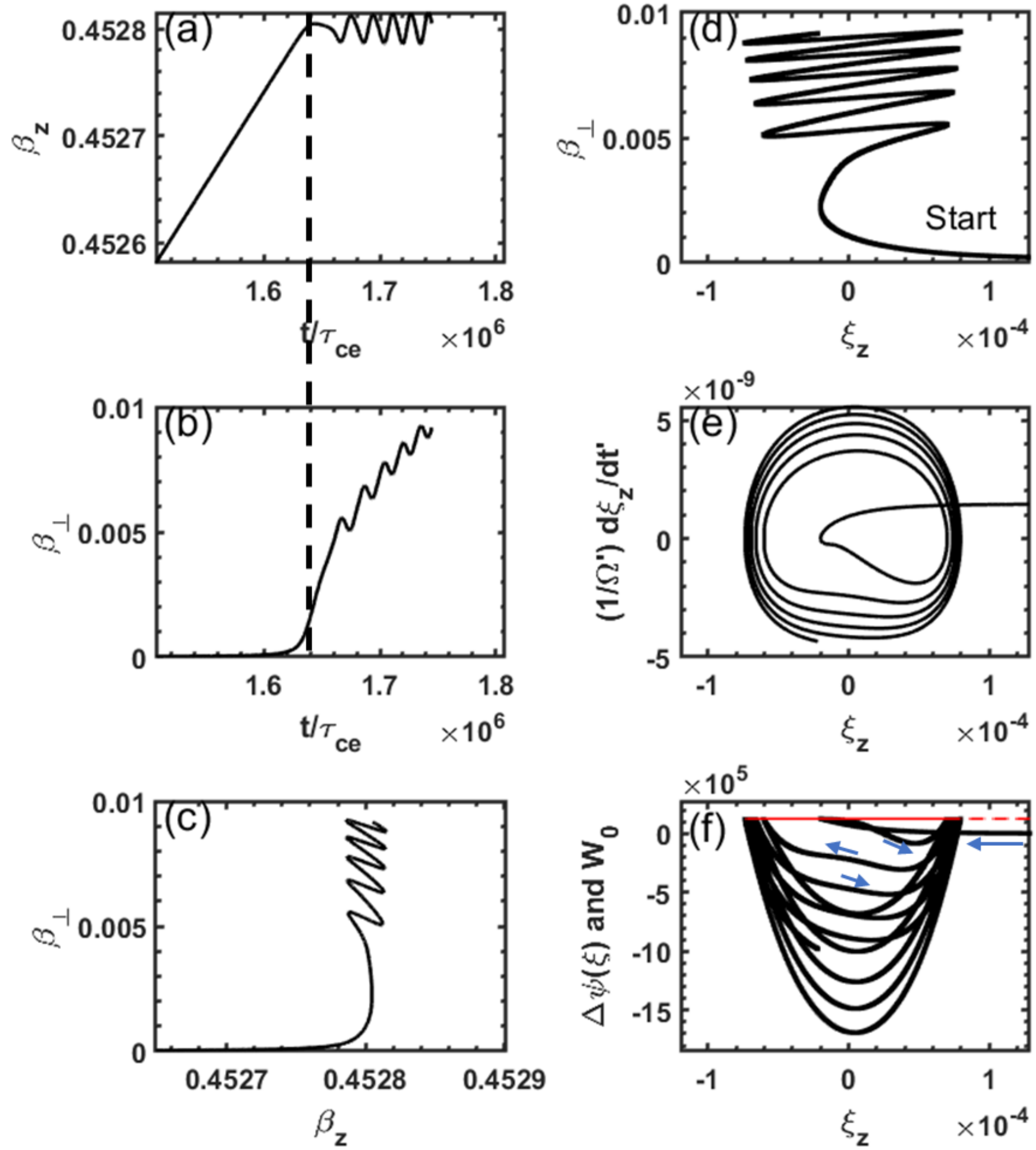

Figure 2. Same as Fig. (1) except with E_W = 22 V/m. This gives $\kappa' = 1.38 \times 10^{-7}$ but same $\frac{\varsigma E_0}{cB_0} = 1.458 \times 10^{-9}$.Panels (e) and (f) are zoom in near the resonant condition $\xi_z = 0$.

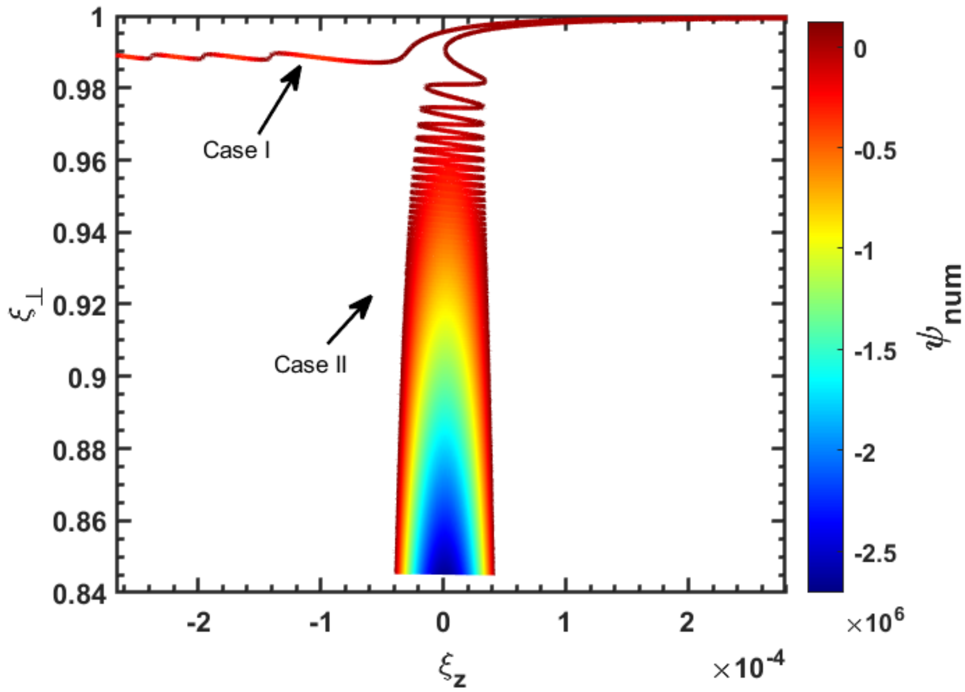

Figure 3. Pseudo-potential $\Delta\psi$ mapped along the electron trajectory in the $(\xi_z, \xi_\perp)$ plane.

Since the pseudo-potential $\Delta\psi(\xi)$ is a function of both β_z and $\beta_\perp$, we traced $\Delta\psi$ along the particle trajectory in the $(\xi_z, \xi_\perp)$ phase space. This approach highlights the underlying structure of the pseudo-potential and enables clearer physical interpretation. As shown in Fig. 3, which compares the two scenarios described in Case I and Case II. It can be seen that when the electron becomes trapped under the resonant condition, it slips into a “deep potential valley” that extends further along the $\xi_\perp$ direction. In contrast, if the electron passes through the resonant region without being trapped, it continues on a “highway”-like trajectory without further obstruction.

To determine the critical boundary of the trapping region, we refer to Eq. (45)and Eq.(52). Assuming the initial perpendicular velocity is approximately zero ($\beta_{\perp 0} = 0$), then s =0. Under this condition, the dynamics are governed solely by two coefficients: κ' and $\frac{\varsigma E_0}{cB_0}$, ξ_{z0} is inconsequential provided it lies outside of resonant region, as demonstrated in Fig.2 (e) and (f), where the ξ_z is mainly shifted by static electric field before the resonance at $\xi_z = 0$. As shown in Fig. 4, the trapping region is indicated in yellow, while the blue region corresponds to the passing regime. Case I and Case II are marked with star symbols in the figure, located in the passing and trapping regions, respectively. For special case as given in Fig.1, where $\frac{\varsigma E_0}{cB_0} = 1.458 \times 10^{-9}$, the critical threshold is $\kappa_c' = 1.367 \times 10^{-7}$, and $\frac{E_{\perp c}}{E_0} = \frac{\kappa_c' \gamma_T c B_0}{n E_0} \approx 102$. Consequently, effective electron trapping in the electromagnetic wave requires the LCP electric field intensity to exceed the background static electric field by a factor of more than 102 in typical tokamak plasma with frequencies near the upper-hybrid mode.

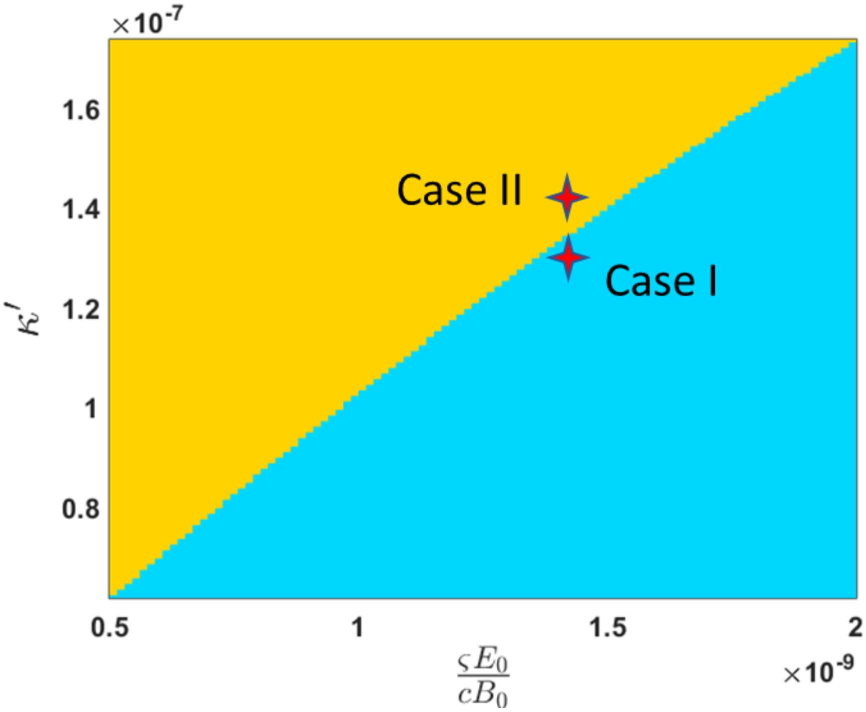

Figure 4. Parameter space of ($\frac{\varsigma E_0}{cB_0}$, κ') showing electron trapping (yellow) and passing (blue) regimes.

IV. Benchmark with quantum theory

One characteristic worth pointing out is that when the electron is trapped in the electromagnetic wave, the energy transfer from the static electric field to the gyrokinetic energy is governed by quantum theory (QE theory) [29]

$$\eta_{\perp} = \frac{n|\Omega|/\gamma_c}{k \cdot v} \tag{63}$$

Here γ_c refers to the Lorentz factor during the resonance. For anomalous Doppler resonance, n = 1 and $k \cdot v = \omega + |\Omega|/\gamma_c$, η_p can be written as

$$\eta_p = \frac{1}{1 + |\omega/\Omega|\gamma_c} \tag{64}$$

For Case II, $\frac{\omega}{\Omega} = -1.1$ and $\gamma_c = 1.1215$ we have $\eta_{\perp}$ =0.448. To numerically calculate the energy transfer ratio, we evaluate the work done by the static electric field during resonance:

$$W_E = \int_0^t E_0 q v_z dt - \int_0^{t_c} E_0 q v_z dt \tag{65}$$

Here τ_c refers to the beginning of trapping condition. Before the trapping condition where $t < \tau_c$, The work done by the static electric field is expressed as:

$$\mathrm{W_E} = \int_0^t E_0 q v_z dt \tag{66}$$

The increase of perpendicular energy is given by

$$\mathrm{W}_\perp = \frac{1}{2} m v_\perp^2 \tag{67}$$

Since the $\mathrm{W}_\perp \approx 0$ before the resonance happen, we can use the $\mathrm{W}_\perp$ directly as the increasement from the resonant condition. Finally, the energy transfer ratio is calculated as $\eta_\perp = W_\perp / W_E$.

The energy transfer ratio from the static electric field to parallel kinetic energy is :

$$\eta_\parallel = \frac{W_\parallel}{W_E} \tag{68}$$

Here $\mathrm{W}_\parallel = \frac{1}{2} m v_\parallel^2 - \frac{1}{2} m v_0^2$ before $t < \tau_c$ where v_0 refers to the initial velocity and $\mathrm{W}_\parallel = \frac{1}{2} m v_\parallel^2 - \frac{1}{2} m v_c^2$ after $t > \tau_c$ after where v_c refers to the resonant velocity .

The $\eta_\perp$ values obtained from the two methods are illustrated in Fig.5. As the electron is trapped by electromagnetic wave ($t > t_c$ with $t_c \approx 1.67\tau_{ce}$), the energy transfer ratio from the numerical results tends to approach the theoretical prediction. Beside this, the parallel energy transfer ratio is 100% before resonant condition and then is 0 during the resonant condition. The other 55% energy will transfer to the stimulated wave emission as described in quantum description[29]. The agreement between the numerical and theoretical results confirms both the accuracy of the simulation and the consistency between quantum theory and classical dynamics.

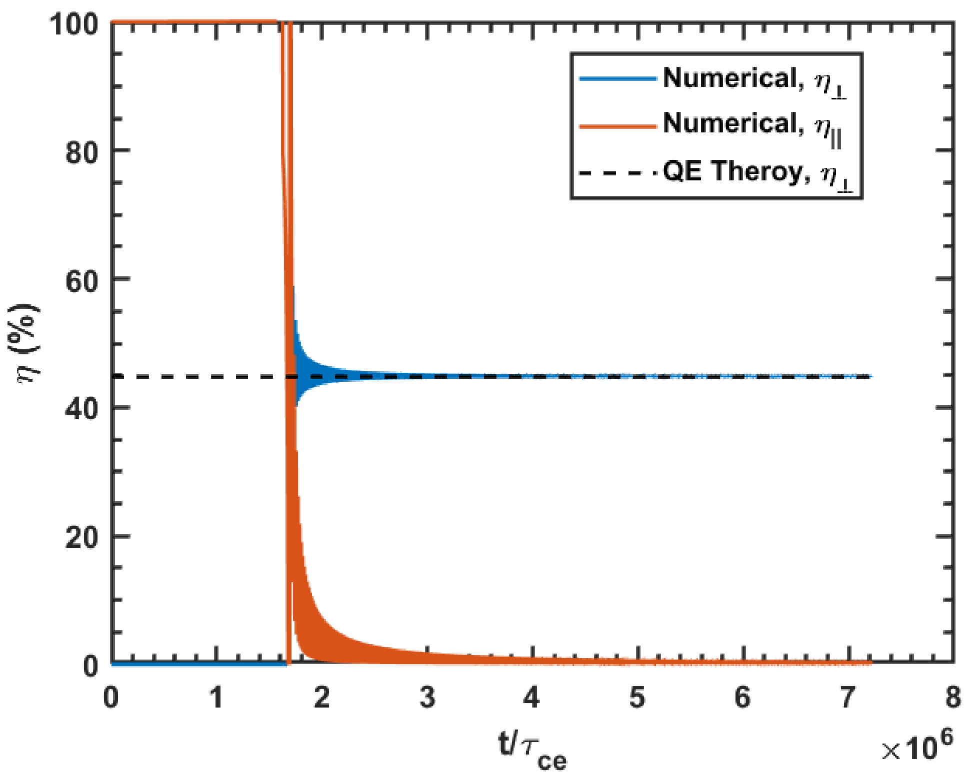

Figure 5. Energy transfer ratio from the static electric field to the gyrokinetic energy $\eta_\perp$ and parallel kinetic energy $\eta_\parallel$. The parameters used here are the same as in Fig. 2 (QE theory means theory based on quantum equation).

V. Discussion

This trapping effect can be qualitatively understood through the conservation of angular momentum and linear momentum[27]. We can draw an analogy by treating the cyclotron electron as a system that contains both internal and kinetic energy, where the internal energy refers to gyrokinetic energy and kinetic energy refers to its translational motion along the magnetic field. When this system is stimulated by an external E.M wave, it undergoes stimulated emission, radiating E.M wave identical to the external one.

For anomalous doppler resonance, Since the emitted E.M wave propagates in the same direction as the electron, conservation of linear momentum requires the electron to lose some of its parallel momentum. At the same time, because the electron possesses right-hand circularly rotation (associated with positive angular momentum), while the emitted wave has left-hand circularly polarization (associated with negative angular momentum), conservation of total angular momentum requires the electron to gain angular momentum after emission. As a result, the electron loses kinetic energy and gains gyrokinetic energy. However, a static electric field continues to replenish the lost kinetic energy. When the rate of energy loss to the E.M wave balances the energy input from the electric field, the electron's parallel velocity ceases to increase, and the electron becomes trapped in the electromagnetic wave. This manifests as a continuous transfer of energy from the static electric field to the gyrokinetic energy of the system.

The redistribution of electron energy between parallel motion and gyrokinetic energy suggests a possible route for mitigating runaway electrons. Tailored wave injections (e.g., whistler-mode or electron cyclotron waves) could induce resonant trapping, helping to suppress runaway electrons. At the same time, the continuous energy transfer from static electric fields to gyrokinetic energy may provide a novel pathway for plasma heating, complementing established methods such as electron cyclotron resonance heating (ECRH). These effects merit further investigation within the framework of wave–plasma interactions.

VI. Summary

In conclusion, trapping under anomalous Doppler resonances is analyzed via the pseudo-potential approach. The parallel velocity oscillates within a potential well, while the perpendicular velocity grows continuously. Critical trapping energy is obtained numerically, with energy conservation ratios from simulations and quantum theory showing strong agreement. The underlying mechanism is explained in terms of angular and linear momentum conservation, and potential applications for runaway electron suppression and plasma heating are discussed.

Appendix:

a. Prove the relationship between resonant condition and ξ_z

The parameter ξ characterizes the frequency mismatch relative to the resonance condition given by

$$\omega = \boldsymbol{k} \cdot \boldsymbol{v} + g\frac{\Omega}{\gamma} \tag{69}$$

This relationship can be derived as follows: Starting from the definition of ς as shown in Eq.(44), we have:

$$\varsigma\beta_z' = \frac{\omega}{\Omega}\frac{n}{\gamma_T}\gamma'\beta_z' \tag{70}$$

Since $\{\gamma\beta, \gamma\}$ are four-vector, we have

$$\gamma'\beta_z' = \gamma_T(\gamma\beta_z - \beta_T\gamma) = \gamma_T\gamma\left(\beta_z - \frac{1}{n}\right) \tag{71}$$

Substituting Eq. (71) and Eq. (70) into Eq. (13) gives

$$\xi_z = 1 + g\frac{\omega}{\Omega}\frac{n}{\gamma_T}\gamma_T\gamma\left(\beta_z - \frac{1}{n}\right) = g\frac{g\frac{\Omega}{\gamma} + k \cdot v - \omega}{\frac{\Omega}{\gamma}} \tag{72}$$

Here $g\frac{\Omega}{\gamma} + k \cdot v - \omega = 0$ represents the resonant condition.

References

[1] Golovanivsky K S 1982 The Gyrac - a Proposed Gyro-Resonant Accelerator of Electrons *Ieee T Plasma Sci* **10** 120-9

[2] Gal O 1989 GYRAC: a compact, cyclic electron accelerator *Ieee T Plasma Sci* **17** 622-9

[3] Shprits Y Y, Runov A and Ni B 2013 Gyro‐resonant scattering of radiation belt electrons during the solar minimum by fast magnetosonic waves *Journal of Geophysical Research: Space Physics* **118** 648-52

[4] Pukhov A, Sheng Z M and Meyer-ter-Vehn J 1999 Particle acceleration in relativistic laser channels *Physics of Plasmas* **6** 2847-54

[5] Bai M, Lee S, Glenn J, Huang H, Ratner L, Roser T, Syphers M and Van Asselt W 1997 Experimental test of coherent betatron resonance excitations *Physical Review E* **56** 6002

[6] Baartman R 1995 Betatron resonances with space charge *Proceedings of Space Charge Physics in High Intensity Hadron Rings (Shelter Island, New York, USA, 1998)*

[7] Tajima T and Dawson J M 1979 Laser Electron-Accelerator *Physical Review Letters* **43** 267-70

[8] Yu W, Yu M, Ma J, Sheng Z, Zhang J, Daido H, Liu S, Xu Z and Li R 2000 Ponderomotive acceleration of electrons at the focus of high intensity lasers *Physical Review E* **61** R2220

[9] Gary S P, Montgomery D and Swift D W 1968 Particle Acceleration by Electrostatic Waves with Spatially Varying Phase Velocities *Journal of Geophysical Research* **73** 7524-+

[10] Sheena Z, Ruschin S, Gover A and Kleinman H 1990 High-Efficiency Nonadiabatic Trapping of Electrons in the Ponderomotive Potential Wells of Laser Beats *Ieee J Quantum Elect* **26** 203-6

[11] Mozer F, Agapitov O, Giles B and Vasko I 2018 Direct observation of electron distributions inside millisecond duration electron holes *Physical Review Letters* **121** 135102

[12] Grach V S, Artemyev A V, Demekhov A G, Zhang X J, Bortnik J, Angelopoulos V, Nakamura R, Tsai E, Wilkins C and Roberts O W 2022 Relativistic electron precipitation by EMIC waves: Importance of nonlinear resonant effects *Geophysical Research Letters* **49** e2022GL099994

[13] Millan R and Baker D 2012 Acceleration of particles to high energies in Earth’s radiation belts *Space Science Reviews* **173** 103-31

[14] Bellan P M 2013 Pitch angle scattering of an energetic magnetized particle by a circularly polarized electromagnetic wave *Physics of Plasmas* **20**

[15] Bourdier A and Gond S 2000 Dynamics of a charged particle in a circularly polarized traveling electromagnetic wave *Physical Review E* **62** 4189-206

[16] Liu H, He X, Chen S and Zhang W 2004 Particle acceleration through the resonance of high magnetic field and high frequency electromagnetic wave *arXiv preprint physics/0411183*

[17] Nusinovich G S, Korol M and Jerby E 1999 Theory of the anomalous Doppler cyclotron-resonance-maser amplifier with tapered parameters *Physical Review E* **59** 2311

[18] Nusinovich G S, Latham P and Dumbrajs O 1995 Theory of relativistic cyclotron masers *Physical Review E* **52** 998

[19] Qian B L 1999 An exact solution of the relativistic equation of motion of a charged particle driven by a circularly polarized electromagnetic wave and a constant magnetic field *Ieee T Plasma Sci* **27** 1578-81

[20] Qian B L 2000 Relativistic motion of a charged particle in a superposition of circularly polarized plane electromagnetic waves and a uniform magnetic field *Physics of Plasmas* **7** 537-43

[21] Roberts C S and Buchsbaum S 1964 Motion of a charged particle in a constant magnetic field and a transverse electromagnetic wave propagating along the field *Physical Review* **135** A381

[22] Weyssow B 1990 Motion of a single charged particle in electromagnetic fields with cyclotron resonances *Journal of plasma physics* **43** 119-39
[23] Mozer F, Agapitov O, Krasnoselskikh V, Lejosne S, Reeves G and Roth I 2014 Direct observation of radiation-belt electron acceleration from electron-volt energies to megavolts by nonlinear whistlers *Physical review letters* **113** 035001
[24] Artemyev A, Agapitov O, Mozer F and Krasnoselskikh V 2014 Thermal electron acceleration by localized bursts of electric field in the radiation belts *Geophysical Research Letters* **41** 5734-9
[25] Liu C, Hirvijoki E, Fu G-Y, Brennan D P, Bhattacharjee A and Paz-Soldan C 2018 Role of kinetic instability in runaway-electron avalanches and elevated critical electric fields *Physical Review Letters* **120** 265001
[26] Xie Z-K, Zong Q-G, Yue C, Zhou X-Z, Liu Z-Y, He J-S, Hao Y-X, Ng C-S, Zhang H and Yao S-T 2024 Electron scale coherent structure as micro accelerator in the Earth's magnetosheath *Nature Communications* **15** 886
[27] Xu X, Xie J, Liu J and Liu W 2025 Analysis of the Anomalous Doppler Effect from Quantum Theory to Classical Dynamics Simulations *Chinese Physics B* **34** 120301
[28] Pokol G, Kómár A, Budai A, Stahl A and Fülöp T 2014 Quasi-linear analysis of the extraordinary electron wave destabilized by runaway electrons *Physics of Plasmas* **21**
[29] Nezlin M V 1976 Negative-energy waves and the anomalous Doppler effect *Soviet Physics Uspekhi* **19** 946